

EXPERIMENTAL AND NUMERICAL INVESTIGATION OF 3D PRINTED ELASTOMERIC COMPOSITE WITH INTEGRATED SMA ACTUATOR

**ZHENBI WANG^{1*}, ACHYUTH R. ANNADATA², ANJA WINKLER¹, RAINER
BARTH¹, ANETT ENDESFELDER³, CHOKRI CHERIF², MARTINA
ZIMMERMANN³, NIELS MODLER¹**

¹Institute of Lightweight Engineering and Polymer Technology (ILK)
Technische Universität Dresden, Dresden, Germany

² Institute of Textile Machinery and High Performance Material Technology (ITM)
Technische Universität Dresden, Dresden, Germany

³ Institute of Materials Science (IfWW)
Technische Universität Dresden, Dresden, Germany

* Corresponding author (zhenbi.wang@tu-dresden.de)

Abstract. Shape memory alloys (SMAs) have been widely used to manufacture soft functionally integrated structures by embedding SMA wires into various soft matrices manufactured by conventional molding methods or 3D-printing technologies. 3D printing enables rapid prototyping, custom design as well as manufacturing of parts with complex structures and high resolutions. This article presents a 3D printed elastomeric composite with integrated SMA wire. The matrix of the composite was printed using thermoplastic polyurethane (TPU), with the SMA wire embedded during the 3D printing process. While the SMA is being excited, the deformation of the specimen was measured optically using DIC (Digital Image Correlation) and simulated using ANSYS. This research offers a promising approach for developing SMA-based elastomeric composites with customized shapes, sizes, and performance characteristics.

Key words: Elastomeric composite, Shape memory alloy, 3D printing, Soft actuator, Smart materials, Rapid prototyping, Finite element modeling

1 INTRODUCTION

Smart materials, also known as intelligent or responsive materials, have gained growing interest in recent years due to their ability to sense stimuli, recognize information and respond accordingly [1]. Soft smart materials are particularly noteworthy because they retain these characteristics while being flexible and lightweight. For example, they can realize high deformability and controllable surface morphology that mimics biological touch [2]. Additionally, they are

easy to prepare and hold great promise for use in diverse applications such as medical treatment, bionics, and soft robotics [3].

A popular method for the creation of soft smart materials is the embedding shape memory alloys (SMAs) into soft matrices [4]. SMAs are capable of returning to their original shape after being deformed by an external stimulus, such as temperature or stress. Compared to other smart materials like piezoceramics [5], electrostrictives [6] and dielectric elastomers [7], they are ideal for producing adaptive structures that respond quickly and can handle large deflections while transmitting high forces [8]. Furthermore, Wire-shaped SMAs are readily available in a wide range of commercial varieties. Functionally integrated structures with high performance could be manufactured by combining SMA wires with soft matrices. There are two primary techniques for embedding SMA wires into soft matrices: conventional molding and 3D printing [4]. Conventional molding involves using molds to create soft matrices with embedded SMA wires, but this method is limited by the complexity of the mold and customization difficulties. On the other hand, 3D printing generates parts directly from computer graphics data without requiring any mechanical processing or tools. It enables rapid prototyping, custom design, and manufacturing of parts with complex structures and high resolutions [3].

Gilbertson et al. [9] embedded three SMA wires, which serve as driving "muscle lines," into silicone rubber catheter tubing to create an active structure similar to fingers or tentacles. By excitation of the muscle lines with adjusted current, they contract and bend the tubular structure. By controlling the activation and deactivation of the three muscle lines, this structure can bend in three different directions, exhibiting smooth and realistic motion. A biomimetic soft robot resembling a caterpillar is described in [10]. This robot is manufactured by molding silicone rubber in 3D printed molds. A pair of SMA coil actuators are installed in the longitudinal cavity on the ventral side of the robot body, controlling the crawling motion of its front and rear parts. Rolling can be achieved by rapidly contracting this pair of SMA coils. A comparable study, referenced as [11], also utilized SMA coil actuators embedded in longitudinal cavities of a soft silicone tentacle like structure. However, unlike the robotic caterpillar, they directly 3D printed the tentacle-like structure using soft elastomeric material, thereby eliminating the need for molding. Deng et al. [12] developed a robotic hand using coil actuators. They used fully 3D printed flexible thermoplastic polyurethane (TPU) to construct the hand, and embedded two SMAs into each finger to control their bending and stretching. By changing the material distribution at the joint to reduce its stiffness, larger joint deformation was achieved. When electrically heated, the SMA coil actuators used in [10] and [12] provide significantly greater contraction force compared to the muscle wire actuators described earlier, thus providing greater movement [11]. In the above-mentioned studies, it was observed that the SMA wires were not completely integrated into the matrix. Instead, they functioned as two distinct systems - one providing mechanical structure and the other generating contraction force in a specific direction. These systems were manufactured separately and then linked together through suitable mechanisms. The desired movement was attained by altering the number and placement of SMA actuators while also regulating their activation and deactivation.

Lohse et al. [8] developed a novel type of actively deformable composites by knitting SMA

wires into glass fiber fabrics and impregnating them with liquid silicone rubber. By adjusting the knitting pattern, they were able to modify the stiffness of the composite material [13]. Driven by SMA wires, the material structure with flexible middle section and stiff sides can achieve a joint-like motion [13]. Mersch et al. [14] overbraided the SMA wire with copper wires and polyamide yarns, which formed a core-sheath structure, and sewed it onto a glass fiber woven in a U-shaped pattern using a tailored fiber placement (TFP) machine, and finally impregnated the textile with silicone. The temperature of the SMA wire can be monitored by the resistance change of the copper wire in the braid tube wrapped around the SMA wire to achieve closed-loop control. In [8, 13, 14], SMA wires were fully integrated into the matrix material to create a soft intelligent composite. This eliminates the need for subsequent installation of SMA wires and allows for more complex movements by adjusting the configurations of different components within the composite material.

Inspired by these studies, the present study is dedicated to developing a composite material in which SMA wires will be directly integrated using 3D printing technology. Thus, TPU was selected as matrix material and specific specimen were manufactured using 3D-printing technology. The deformation of the specimen during excitation were evaluated using Digital Image Correlation (DIC). Additionally, ANSYS simulation was conducted to predict the deformation behavior of such composite. These findings will enhance the understanding of the developed composite material and improve its design for future applications.

The remaining parts of this article are organized as follows. Section 2 describes the materials used, the specimen design and manufacturing method, as well as the design of a suitable test bench for proper excitation and optical characterization. Section 3 presents the results simulated in ANSYS and experimental results obtained using DIC testing. Section 4 proposes conclusions and suggestions for future work.

2 MATERIALS AND METHODS

2.1 Deformation mechanism of SMA-driven composite material

The presented study utilized Nitinol wires (SmartFlex[®] 300 μm) with a diameter of 0.3 mm, which is a SMA material provided by SAES Getters (20045 Lainate (Milan), Italy). The wires were trained in a pre-strained status which allows for two-way shape memory effect (TWSME) through thermal activation. The TWSME is a phenomenon where shape memory materials can change their shape between two predefined shapes under different temperature or stress conditions. The used SMA wire has a pre-strain of approximately 4%, with an austenite start and finish temperatures of 58.7 °C and, 80.5 °C respectively. The TWSME helps in recovering two different shapes, making it very useful for applications that require repeated switching of shapes.

The 3D printed specimen matrix was made using TPU filament (TPU Flex Semisoft) with a hardness of A88 provided by Filamentworld (89231 Neu-Ulm, Deutschland). Based on the data sheet provided by the manufacturer, this material has a relatively high softening temperature of 98 °C, as determined using the VICAT A (VST) test method according to ISO 306, and will

not soften at the excitation temperature of the SMA wire used. It is also flexible enough to accommodate the deformation of heated SMA, and can provide some recovery elasticity to accelerate sample recovery to its original state when SMA is cooled down.

In the presented work, the SMA wire was overbraided by utilizing a similar approach to [14]. The overbraided SMA wire was embedded in the TPU matrix at the position deviating from the neutral plane (as shown in Figure 1.) One side of the TPU matrix was fixed like a bending beam, while both ends of the SMA wire outside the TPU matrix were stretched and fixed. When the SMA wire is heated by current to its phase change temperature and shortened, it drives the bending of the whole specimen. Since the braided tube surrounding the SMA wire is flexible and the SMA wire can slide inside the tube, so the shortening of the SMA does not damage the structure of the TPU matrix. The flexible braided tube does not increase the stiffness of the TPU substrate, making it difficult to bend.

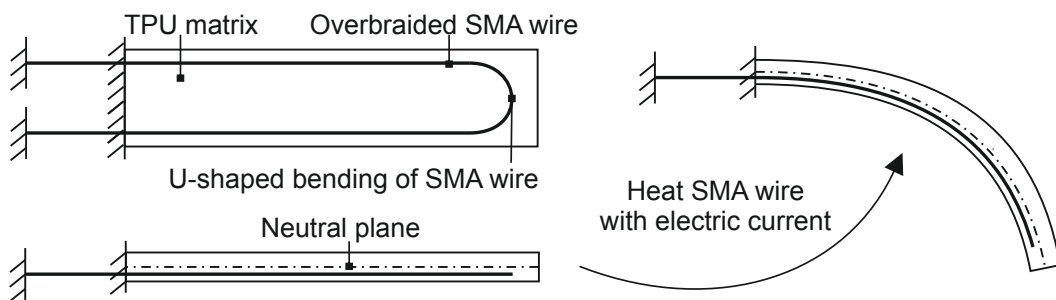


Figure 1: Deformation mechanism of the proposed SMA-driven composite material

2.2 Manufacturing process of the composite specimen

The manufacture of the composite sample consists of three main steps as shown in Figure 2: overbraiding the SMA wire with copper wires and polyamide yarns, embedding the overbraided SMA wire during the 3D printing process of TPU matrix, and establishing mechanical and electrical connections of the sample. As shown in Figure 2a, the SMA wire was overbraided with copper wires and polyamide yarns as described by Mersch, et al. [14].

Compared to the commonly used rigid PLA filament, TPU filament is more difficult to print. The main reason for this is that TPU is a flexible material that is prone to deformation. The part of the filament between the extruder gears and the print head is compressed and stretched during the extrusion and retraction process, resulting in the pressure inside the print head not being adjusted in time and causing a delayed material flow, as shown in Figure 3. This can be improved by reducing the printing speed, using larger nozzle on the print head and decreasing clamping force between extruder gears. In addition, reducing the distance between the extruder and the print head can effectively minimize material flow delays, so direct-drive 3D printers are often used for printing flexible materials such as TPU.

Moreover, TPU Filament is very sensitive to fast and sudden movements. Too fast retraction speed and too large retraction distance can easily lead to clogging of the print head nozzle or

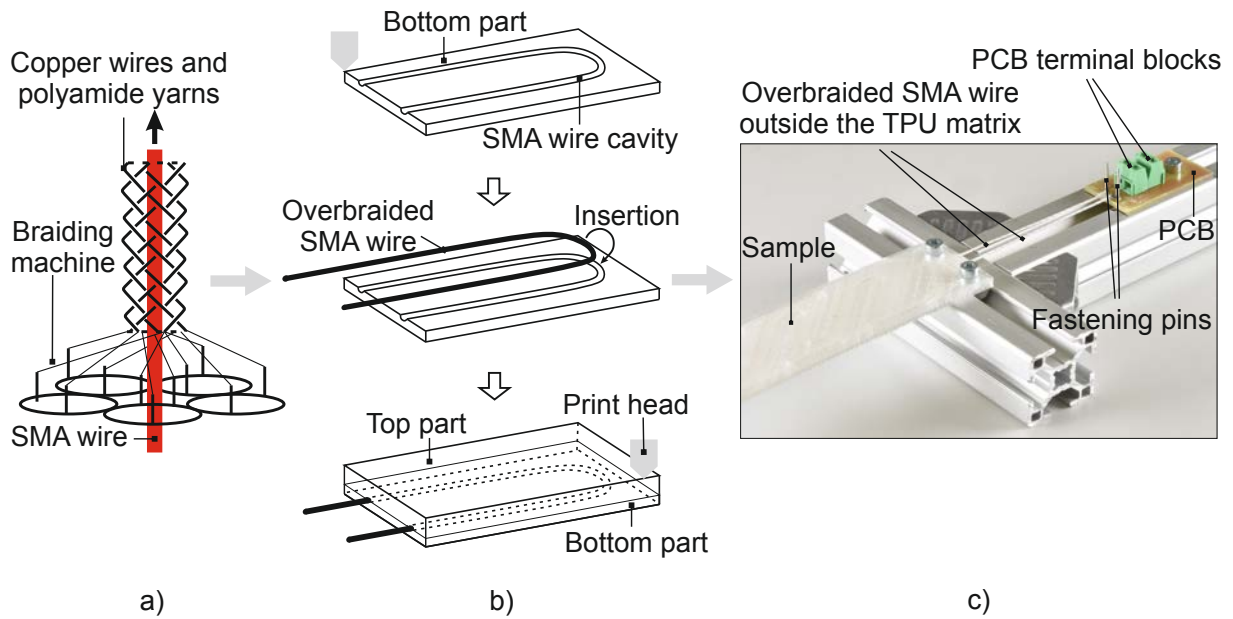


Figure 2: The process of manufacturing specimens: a) Overbraiding the SMA wire with copper wires and polyamide yarns; b) Embedding the overbraided SMA wire during the 3D printing process of TPU matrix; c) Establishing mechanical and electrical connections of the specimen.

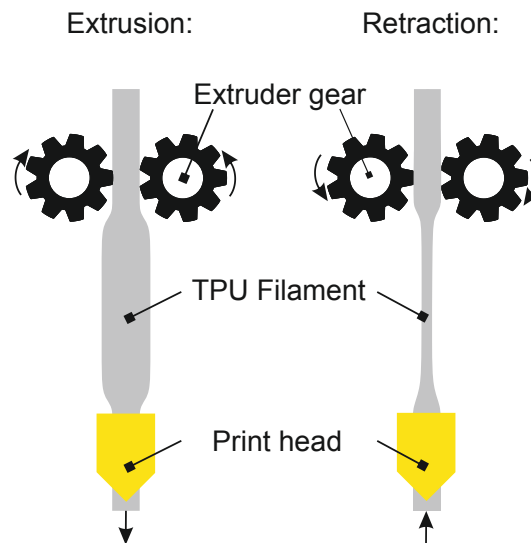


Figure 3: Deformation of the flexible TPU filament during extrusion and retraction.

insufficient subsequent extrusion, so retraction was not set in this study. As the TPU filament used in this study have a medium hardness (A88) and the problems above mentioned are not significant, a Bowden-tube 3D printer Creality Ender 3 Pro was used for manufacturing the specimen.

After calibration experiments, it was concluded that good quality specimens could be printed by generating G-code in Ultimaker Cura 5.1.0 according to the setting parameters in Table 1. Other settings are left as default.

Table 1: Print settings in Ultimaker Cura 5.1.0

Parameter name	Value	Parameter name	Value
Layer Height	0.16 mm	Infill Pattern	Grid
Wall Thickness	1.2 mm	Printing Temperature	220 °C
Wall Line Count	3	Build Plate Temperature	30 °C
Top/Bottom Thickness	0.84 mm	Print Speed	20 mm/s
Top/Bottom Layers	6	Disable Retraction	
Infill Density	20 %	Disable Print Cooling	

The TPU matrix was designed using SOLIDWORKS, with the cavity for embedding the overbraided SMA wire cut out. The diameter of the cavity is 1.3 mm, slightly larger than that of the overbraided SMA wire (0.98 mm), considering the shrinkage of the material. Figure 4 shows the dimensions of the specimen, the shape and location of the SMA wire, as well as a photo of the printed sample. To integrate the overbraided SMA wire into the TPU matrix, a post-

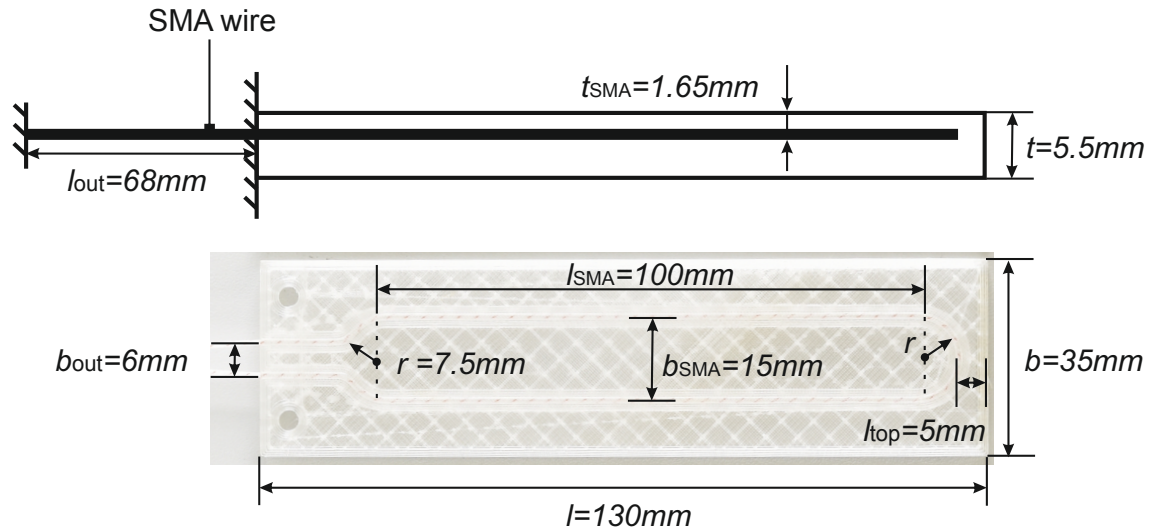


Figure 4: The specimen size and the position of the U-shaped SMA wire within it.

processing script called "Pause at Height" was utilized in the slicing software to temporarily halt 3D printing of the sample at the second-to-last layer of the cavity. The SMA wire was then inserted into this empty cavity. After that, the printing of the remaining part was resumed.

As stated in Section 2.1, it is necessary to pre-stretch and secure both ends of the SMA wire and connect them to the power supply. To ensure more reliable connections by separating mechanical and electrical connections, a printed circuit board (PCB) is utilized as depicted in Figure 2c. The two ends of the SMA wire were wrapped around the fastening pins on the PCB and secured with glue. The top ends of the SMA wire are then inserted into terminal blocks on the PCB for connection to the power supply. Additionally, there is a hole on the PCB that allows screws and nuts to be used for fixing it onto a metal frame or a 3D printed part.

2.3 Test bench set-up

In order to describe the coupling between the specimen matrix structure and the SMA wire, the deformation and deflection of the specimen must be determined. For this purpose, a test bench was set up for optically measuring the deformation of specimens using digital image correlation (DIC), as shown in Figure 5. A pair of DIC cameras was positioned in front of the sample to capture its deformation data from the side. The test bench consists of a metal profile frame, screws/nuts, 3D-printed parts, and a spring. Its main function is to hold the specimen in place, apply a quantitative pre-stretch force to the SMA wire, and provide power to it. The upper and lower sliders are connected by a spring and their relative displacement is equal to the extended length of the spring.

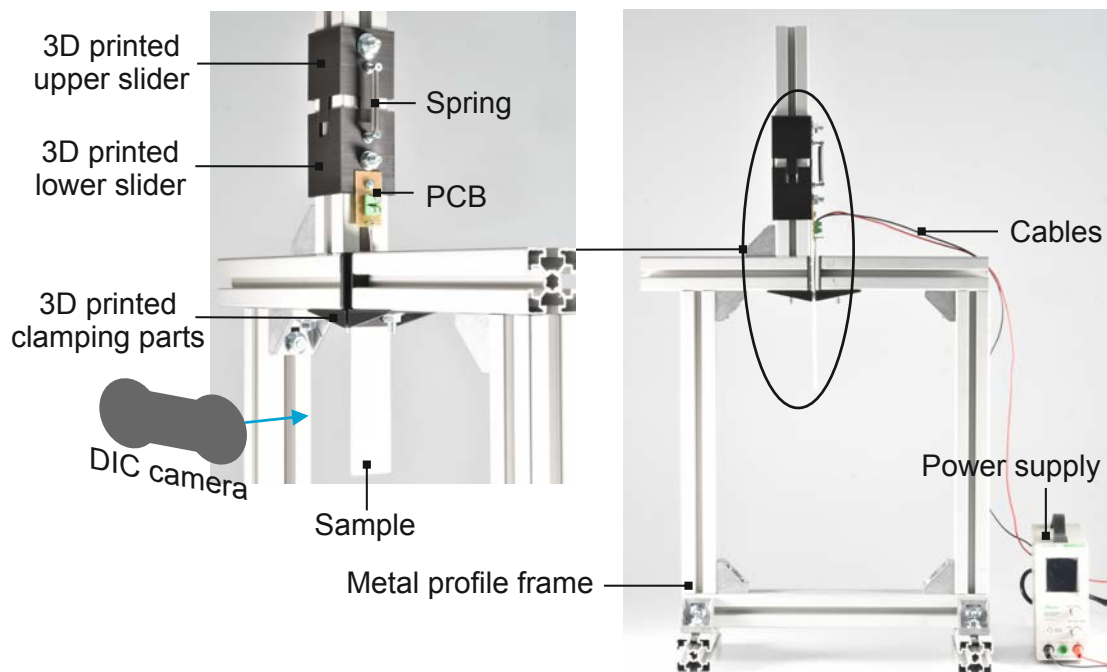


Figure 5: Photographs of the test bench: On the left side, detail of the test bench showing the fixation of the specimen; On the right side, overview of the bending test bench.

Firstly, the specimen was fixed between the 3D-printed clamping parts and then fixed together onto the metal frame. Subsequently, the PCB board was attached to the lower slider. By pulling the upper slider upwards, tension was applied to the spring which results in pre-stretch force being applied to the SMA wire. To ensure that the pre-stretch force applied in each experiment is consistent, the relative displacement corresponding to a pre-stretch force of 5.9 N is marked on the lower slider. When the upper slider is pulled to this marked point, the screw on the lower slider was tightened onto the metal frame, thus applying a constant pre-stretch force to the SMA wire. In addition, the PCB board is connected to the positive and negative poles of the power supply through two cables.

3 RESULTS

3.1 Simulation results

Modeling and simulation of the SMA-driven TPU specimen was conducted using ANSYS Workbench. Multi-linear isotropic hardening was used to capture the plastic deformation in TPU. Plastic stress and strain were determined based on uni-axial tensile tests. In conventional SMA simulation studies, a stretch force must be applied to the SMA in advance to induce strain, and then the temperature is applied to simulate its contraction deformation, achieving one-way shape memory effect (OWSME). Therefore, only straight SMA wires can be modeled because it is almost impossible to pre-stretch a bent SMA wire while keeping its shape unchanged. To address this problem, Woodworth et al. [15] developed a user-defined material model for SMA. This material model was developed to determine the behaviour of SMA under mechanical loading by considering functional fatigue and transformation induced plasticity. The pre-stretching is already included in the material model to assign a strain in the SMA before solving for shape memory effect. Therefore, there is no requirement of applying stretch force, which makes this model suitable for simulating shaped SMA wires. In the present study, this SMA material model was applied to the simulation. The SMA wire and the TPU matrix in the simulation were constrained together at one end and a temperature boundary condition was applied to the SMA wire in a single load step. In addition, the following assumptions were considered during simulation:

- The TPU matrix is considered as a complete solid body, without taking into account the grid infill pattern within it.
- The SMA wire is modeled as a straight wire towards the fixating pins to reduce the non-linearity and computation time, and a "U" bend still exists at the free end of the TPU.
- The TPU is expected to undergo plastic strain due to the high forces exerted by SMA leading to bending deformations. Thus, a consideration in terms of multi-linear isotropic hardening is considered which assumes, that the material response is independent of the direction of loading, by which the first assumption is likely to overcome.

The simulation shows a total deformation of $\delta = 56.998$ mm, as depicted in Figure 6a. Figure 6b displays the volume fraction of martensite inside the SMA wire. Since the specimen

is symmetrical, only half of it is shown in the figure. It can be seen from the figure that the U-shaped bending section of the SMA wire completed a full transformation from martensite to austenite where internal stress was low, whereas about 25 % of martensite remained in the straight sections of the SMA wire where stress was higher. When the bending section is fully deformed, the straight sections have not yet reached their maximum deformation. This indicates that stress can limit or slow down the deformation of SMA wires.

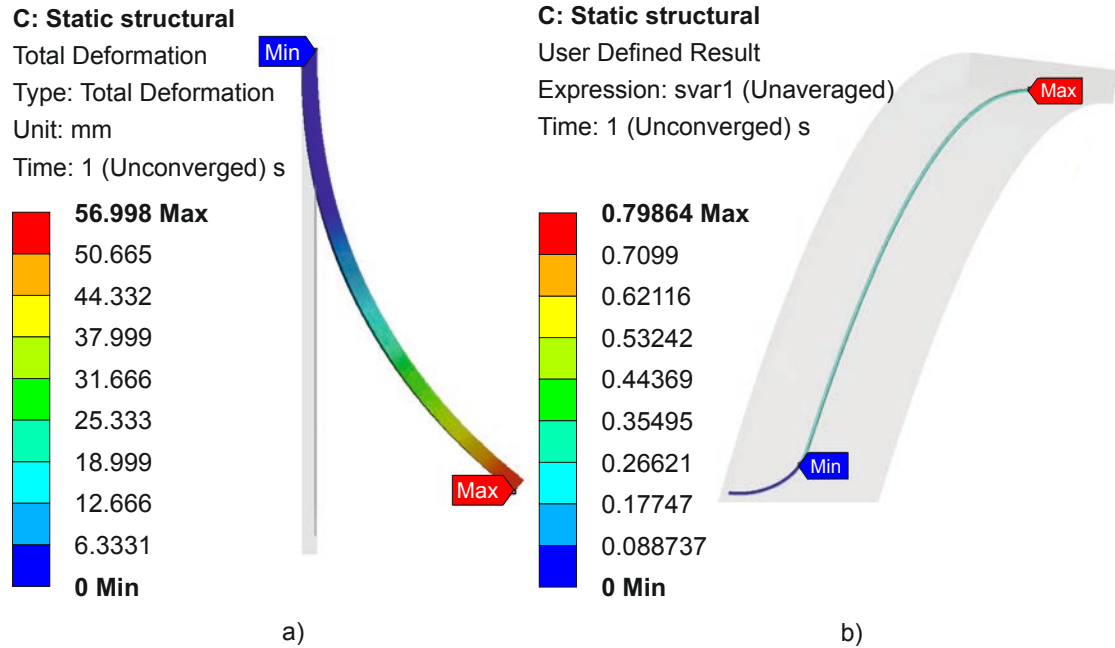


Figure 6: Simulation results obtained using ANSYS workbench: a) total deformation; b) martensite volume fraction.

3.2 Results of deformation tests

The deformation of the specimen was measured using a DIC system. The system employed an ARAMIS 12M (10G) sensor, and the data obtained from the sensor was processed by GOM Testing Controller. Based on pre-tests on the resistance of the SMA wire, it was determined that a voltage of 8.5 V would be appropriate for heating the SMA wire. The chosen settings produced a drive time of 14.6 s.

Figure 7a displays the maximum deflection of the points on the specimen's side from its initial position. The angle and deflections are determined in relation to the fixed points indicated on the test bench. Point A is the midpoint of the bottom edge on the side of the specimen. The angle between the tangent line at point A and the vertical direction is φ . Additionally, there are three deflections measured at point A: δ_X (deflection in x-direction), δ_Y (deflection in y-direction), and δ (total displacement relative to its initial position). Figure 7b and c show how measured values δ , δ_X , δ_Y and φ change over time. Both diagrams indicate an increase in

measured values as the temperature and the phase transition of the SMA wire increase. They increase at a progressively slower rate until reaching their maximum value: $\delta = 90.83$ mm, $\delta_X = 76.58$ mm, $\delta_Y = 48.76$ mm and $\varphi = 81.39^\circ$. The specimens showed similar behavior when reactivated.

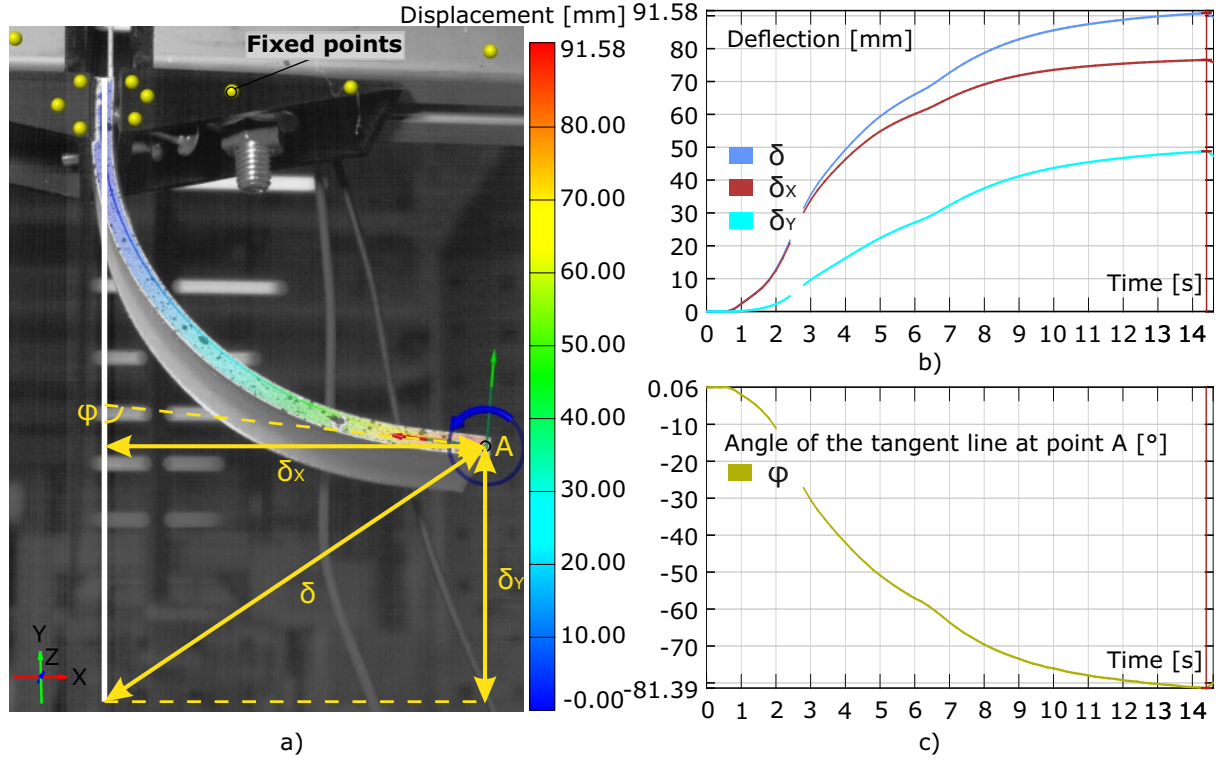


Figure 7: Test results determined by DIC: a) maximum deflection of the points on the side of the specimen from its initial position; b) deflection in x-direction δ_X , deflection in y-direction δ_Y , and the total displacement δ over time at point A; c) Angle between the tangent line at point A and the vertical direction φ over time.

4 DISCUSSION AND CONCLUSIONS

In the presented study, 3D printing technology was utilized to integrate SMA wire into a flexible TPU matrix, developing a novel smart elastomeric composite. Moreover, the braided sensor tube surrounding the SMA wire gives this actuator the ability to self-monitor its own temperature, providing the possibility for closed-loop control of actuator's movement, and allows the SMA wire to slide freely within it, avoiding structural damage.

Due to the use of 3D printing technology, the presented soft actuators can be customized into various shapes and sizes according to the requirements in practical applications. In comparison with conventional molding methods for manufacturing SMA-based smart materials that involve complex processing and assembly procedures, the method described in this article only requires

inserting the SMA wire into reserved cavity during the 3D printing process, which greatly simplifies the manufacturing processes and shortens the manufacturing time.

A large disparity between the simulation and experimental results is noticed and can be attributed to the assumption of considering the solid body for TPU matrix, without the grid infill patterns. Additionally, the material model for SMA was unable to solve further for the non-linearity, leading to convergence problems. This can be confirmed based on the volume fraction of the SMA wire, as the SMA did not completely transform into austenite. The experimental results show that the proposed actuator exhibits repeatable large deformations, indicating that placing SMA wires into soft matrix materials can significantly improve the performance of the soft functional integrated structure.

The powerful driving force of the SMA wire combined with the flexibility of the TPU matrix enables the actuator to withstand larger loads while achieving larger deformations, thereby increasing its application range and flexibility. A potential problem is that high temperatures in the SMA wire can cause the thermoplastic matrix to melt, resulting in structural damage inside the actuator. Therefore, it is important to avoid exciting the SMA wire for long periods of time or at high power. This highlights the importance of detecting the effects of active period and power of the SMA wire on structural damage in future work.

There are many more possibilities for the configuration of soft actuators manufactured using this method. In order to design more complex parts, achieve diverse motion patterns, and improve the control of deformation, there is a need to investigate the effects of material composition and structure to the deformation, such as the properties and spatial distribution of reinforcing materials, the location and shape of shape memory wires, as well as the dimensions and properties of the matrix material. For this purpose, SMA-based smart composites with various configurations will be manufactured using the proposed manufacturing method in the future work and comprehensively characterized by experiments and simulations.

REFERENCES

- [1] M. Su and Y. Song, "Printable smart materials and devices: strategies and applications," *Chemical Reviews*, vol. 122, no. 5, pp. 5144–5164, 2021.
- [2] B. Li, Y.-P. Cao, X.-Q. Feng, and H. Gao, "Mechanics of morphological instabilities and surface wrinkling in soft materials: a review," *Soft Matter*, vol. 8, no. 21, pp. 5728–5745, 2012.
- [3] A. Zolfagharian, A. Z. Kouzani, S. Y. Khoo, A. A. A. Moghadam, I. Gibson, and A. Kaynak, "Evolution of 3d printed soft actuators," *Sensors and Actuators A: Physical*, vol. 250, pp. 258–272, 2016.
- [4] S. Akbari, A. H. Sakhaei, S. Panjwani, K. Kowsari, A. Serjouei, and Q. Ge, "Multimaterial 3d printed soft actuators powered by shape memory alloy wires," *Sensors and Actuators A: Physical*, vol. 290, pp. 177–189, 2019.

- [5] H. Abramovich, “Intelligent materials and structures,” in *Intelligent Materials and Structures*. De Gruyter, 2021.
- [6] Y. Bar-Cohen, *Electroactive polymer (EAP) actuators as artificial muscles: reality, potential, and challenges*. SPIE press, 2004, vol. 136.
- [7] M. Koenigsdorff, J. Mersch, S. Pfeil, and G. Gerlach, “High-strain helical dielectric elastomer actuators,” in *Electroactive Polymer Actuators and Devices (EAPAD) XXIV*, vol. 12042. SPIE, 2022, pp. 149–159.
- [8] F. Lohse, K. Kopelmann, H. Grellmann, M. Ashir, T. Gereke, E. Häntzsche, C. Sennewald, and C. Cherif, “Experimental and numerical analysis of the deformation behavior of adaptive fiber-rubber composites with integrated shape memory alloys,” *Materials*, vol. 15, no. 2, p. 582, 2022.
- [9] R. Gilbertson, “Muscle wires project book, san rafael, ca, usa: Mondo-tronics,” 2000.
- [10] H.-T. Lin, G. G. Leisk, and B. Trimmer, “Goqbot: a caterpillar-inspired soft-bodied rolling robot,” *Bioinspiration & biomimetics*, vol. 6, no. 2, p. 026007, 2011.
- [11] P. Walters and D. McGoran, “Digital fabrication of smart structures and mechanisms—creative applications in art and design,” in *International Conference on Digital Printing Technologies and Digital Fabrication*, vol. 27, no. 2011, 2011, pp. 185–188.
- [12] E. Deng and Y. Tadesse, “A soft 3d-printed robotic hand actuated by coiled sma,” in *Actuators*, vol. 10, no. 1. MDPI, 2020, p. 6.
- [13] F. Lohse, A. R. Annadata, E. Häntzsche, T. Gereke, W. Trümper, and C. Cherif, “Hinged adaptive fiber-rubber composites driven by shape memory alloys—development and simulation,” *Materials*, vol. 15, no. 11, p. 3830, 2022.
- [14] J. Mersch, N. Keshtkar, H. Grellmann, C. A. Gomez Cuaran, M. Bruns, A. Nocke, C. Cherif, K. Röbenack, and G. Gerlach, “Integrated temperature and position sensors in a shape-memory driven soft actuator for closed-loop control,” *Materials*, vol. 15, no. 2, p. 520, 2022.
- [15] L. A. Woodworth, F. Lohse, K. Kopelmann, C. Cherif, and M. Kaliske, “Development of a constitutive model considering functional fatigue and pre-stretch in shape memory alloy wires,” *International Journal of Solids and Structures*, vol. 234-235, p. 111242, 2022.